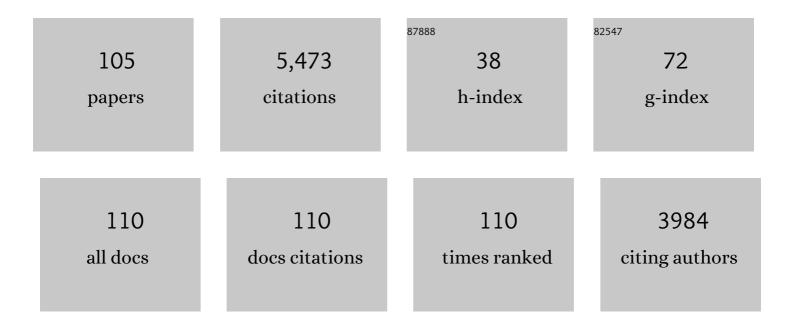
## Keiko Hattori

List of Publications by Year in descending order

Source: https://exaly.com/author-pdf/5629671/publications.pdf Version: 2024-02-01



#	Article	IF	CITATIONS
1	Geochemistry of subduction zone serpentinites: A review. Lithos, 2013, 178, 96-127.	1.4	514
2	Contribution of mafic melt to porphyry copper mineralization: evidence from Mount Pinatubo, Philippines, and Bingham Canyon, Utah, USA. Mineralium Deposita, 2001, 36, 799-806.	4.1	272
3	Tethyan and Indian subduction viewed from the Himalayan high- to ultrahigh-pressure metamorphic rocks. Tectonophysics, 2008, 451, 225-241.	2.2	238
4	Volcanic fronts form as a consequence of serpentinite dehydration in the forearc mantle wedge. Geology, 2003, 31, 525.	4.4	212
5	Adsorption of rare earth elements onto bacterial cell walls and its implication for REE sorption onto natural microbial mats. Chemical Geology, 2005, 219, 53-67.	3.3	211
6	Oxidation Condition and Metal Fertility of Granitic Magmas: Zircon Trace-Element Data from Porphyry Cu Deposits in the Central Asian Orogenic Belt. Economic Geology, 2015, 110, 1861-1878.	3.8	199
7	Evidence of hydration of the mantle wedge and its role in the exhumation of eclogites. Earth and Planetary Science Letters, 2001, 193, 115-127.	4.4	190
8	Geochemical character of serpentinites associated with high―to ultrahighâ€pressure metamorphic rocks in the Alps, Cuba, and the Himalayas: Recycling of elements in subduction zones. Geochemistry, Geophysics, Geosystems, 2007, 8, .	2.5	179
9	Exhumation Processes in Oceanic and Continental Subduction Contexts: A Review. Frontiers in Earth Sciences, 2009, , 175-205.	0.1	170
10	Archean gold mineralization and oxidized hydrothermal fluids. Economic Geology, 1987, 82, 1177-1191.	3.8	154
11	In situ characterization of serpentinites from forearc mantle wedges: Timing of serpentinization and behavior of fluid-mobile elements in subduction zones. Chemical Geology, 2010, 269, 262-277.	3.3	152
12	Serpentinites act as sponges for fluidâ€mobile elements in abyssal and subduction zone environments. Terra Nova, 2011, 23, 171-178.	2.1	125
13	High-sulfur magma, a product of fluid discharge from underlying mafic magma: Evidence from Mount Pinatubo, Philippines. Geology, 1993, 21, 1083.	4.4	121
14	Oxygen isotope ratios of the Icelandic crust. Journal of Geophysical Research, 1982, 87, 6559-6565.	3.3	120
15	Contributions from mafic alkaline magmas to the Bingham porphyry Cu-Au-Mo deposit, Utah, USA. Mineralium Deposita, 2002, 37, 14-37.	4.1	107
16	The Quetico Intrusions of Western Superior Province: Neo-Archean examples of Alaskan/Ural-type mafic–ultramafic intrusions. Precambrian Research, 2006, 149, 21-42.	2.7	101
17	Oxidized sulfur-rich mafic magma at Mount Pinatubo, Philippines. Contributions To Mineralogy and Petrology, 2004, 146, 750-761.	3.1	99
18	Occurrence of arsenic (V) in forearc mantle serpentinites based on X-ray absorption spectroscopy study. Geochimica Et Cosmochimica Acta, 2005, 69, 5585-5596.	3.9	97

Κεικό Ηάττορι

#	Article	IF	CITATIONS
19	Behavior of fluid-mobile elements in serpentines from abyssal to subduction environments: Examples from Cuba and Dominican Republic. Chemical Geology, 2012, 312-313, 93-117.	3.3	94
20	Asthenospheric upwelling, oceanic slab retreat, and exhumation of UHP mantle rocks: Insights from Greater Antilles. Geophysical Research Letters, 2007, 34, .	4.0	87
21	Magma evolution recorded in plagioclase zoning in 1991 Pinatubo eruption products. American Mineralogist, 1996, 81, 982-994.	1.9	85
22	Seafloor hydrothermal clay alteration at Jade in the back-arc Okinawa Trough: mineralogy, geochemistry and isotope characteristics. Geochimica Et Cosmochimica Acta, 1999, 63, 2785-2804.	3.9	80
23	Osmium-isotope ratios of platinum-group minerals associated with ultramafic intrusions: Os-isotopic evolution of the oceanic mantle. Earth and Planetary Science Letters, 1991, 107, 499-514.	4.4	66
24	Sulphur geodynamic cycle. Scientific Reports, 2015, 5, 8330.	3.3	64
25	Helium anomalies suggest a fluid pathway from mantle to trench during the 2011 Tohoku-Oki earthquake. Nature Communications, 2014, 5, 3084.	12.8	58
26	Large Paleozoic and Mesozoic porphyry deposits in the Central Asian Orogenic Belt: Geodynamic settings, magmatic sources, and genetic models. Gondwana Research, 2018, 58, 161-194.	6.0	57
27	The Gandy and Abolhassani Epithermal Prospects in the Alborz Magmatic Arc, Semnan Province, Northern Iran. Economic Geology, 2004, 99, 691-712.	3.8	56
28	Metasomatism of sub-arc mantle peridotites below southernmost South America: reduction of fO2 by slab-melt. Contributions To Mineralogy and Petrology, 2007, 153, 607-624.	3.1	56
29	Subduction of mantle wedge peridotites: Evidence from the Higashiâ€akaishi ultramafic body in the Sanbagawa metamorphic belt. Island Arc, 2010, 19, 192-207.	1.1	55
30	Archaean magmatic sulphate. Nature, 1986, 319, 45-47.	27.8	52
31	Zoned Cr-spinel and ferritchromite alteration in forearc mantle serpentinites of the Rio San Juan Complex, Dominican Republic. Mineralogical Magazine, 2013, 77, 117-136.	1.4	52
32	Halogen (F, Cl, Br, I) behaviour in subducting slabs: A study of lawsonite blueschists in western Turkey. Earth and Planetary Science Letters, 2016, 442, 133-142.	4.4	49
33	D/H ratios, origins, and evolution of the ore-forming fluids for the Neogene veins and kuroko deposits of Japan. Economic Geology, 1979, 74, 535-555.	3.8	44
34	The Hemlo gold deposit, Ontario: A geochemical and isotopic study. Geochimica Et Cosmochimica Acta, 1985, 49, 2041-2050.	3.9	42
35	Corundum-bearing garnet peridotite from northern Dominican Republic: A metamorphic product of an arc cumulate in the Caribbean subduction zone. Lithos, 2010, 114, 437-450.	1.4	42
36	Geochemistry of apatite-rich layers in the Finero phlogopite–peridotite massif (Italian Western Alps) and ion microprobe dating of apatite. Chemical Geology, 2008, 251, 99-111.	3.3	41

Κεικό Ηάττορι

#	Article	IF	CITATIONS
37	A geochemical study on mud volcanoes in the Junggar Basin, China. Applied Geochemistry, 2011, 26, 1065-1076.	3.0	40
38	Calculation of oxygen isotope fractionation between uranium dioxide, uranium trioxide and water. Geochimica Et Cosmochimica Acta, 1982, 46, 1863-1868.	3.9	39
39	Initial geometry of western Himalaya and ultrahigh-pressure metamorphic evolution. Journal of Asian Earth Sciences, 2007, 30, 557-564.	2.3	39
40	Magmatic mineralization and hydrothermal enrichment of the High Grade Zone at the Lac des Iles palladium mine, northern Ontario, Canada. Mineralium Deposita, 2005, 40, 13-23.	4.1	38
41	An atomic level study of rhenium and radiogenic osmium in molybdenite. Geochimica Et Cosmochimica Acta, 2007, 71, 5180-5190.	3.9	38
42	Osmium isotope ratios of PGM grains associated with the Freetown Layered Complex, Sierra Leone, and their origin. Contributions To Mineralogy and Petrology, 1991, 109, 10-18.	3.1	35
43	Geology, Petrology, and Controls on PGE Mineralization of the Southern Roby and Twilight Zones, Lac des Iles Mine, Canada. Economic Geology, 2005, 100, 43-61.	3.8	35
44	Origin of placer laurite from Borneo: Se and As contents, and S isotopic compositions. Mineralogical Magazine, 2004, 68, 353-368.	1.4	35
45	Oxidation state of Paleozoic subcontinental lithospheric mantle below the Pali Aike volcanic field in southernmost Patagonia. Lithos, 2008, 105, 98-110.	1.4	34
46	Titanium- and water-rich metamorphic olivine in high-pressure serpentinites from the Voltri Massif (Ligurian Alps, Italy): evidence for deep subduction of high-field strength and fluid-mobile elements. Contributions To Mineralogy and Petrology, 2014, 167, 1.	3.1	34
47	Origins of ultramafic rocks in the Sulu Ultrahigh-pressure Terrane, Eastern China. Lithos, 2013, 178, 158-170.	1.4	31
48	Volcano–hydrothermal system of Ebeko volcano, Paramushir, Kuril Islands: Geochemistry and solute fluxes of magmatic chlorine and sulfur. Journal of Volcanology and Geothermal Research, 2016, 310, 118-131.	2.1	31
49	Experimental insight into redox transfer by iron- and sulfur-bearing serpentinite dehydration in subduction zones. Earth and Planetary Science Letters, 2017, 479, 133-143.	4.4	27
50	Alteration Mineralogy of the Zhengguang Epithermal Au-Zn Deposit, Northeast China: Interpretation of Shortwave Infrared Analyses During Mineral Exploration and Assessment. Economic Geology, 2021, 116, 389-406.	3.8	27
51	Marine hdrothermal alteration at a Kuroko ore deposit, Kosaka, Japan. Contributions To Mineralogy and Petrology, 1980, 74, 285-292.	3.1	25
52	Sulphur isotope abundances in Aphebian clastic rocks: implications for the coeval atmosphere. Nature, 1983, 302, 323-326.	27.8	25
53	Melt and source mantle compositions in the Late Archaean: A study of strontium and neodymium isotope and trace elements in clinopyroxenes from shoshonitic alkaline rocks. Geochimica Et Cosmochimica Acta, 1996, 60, 4551-4562.	3.9	24
54	Arsenic in a fractured slate aquifer system, New England, USA: Influence of bedrock geochemistry, groundwater flow paths, redox and ion exchange. Applied Geochemistry, 2013, 39, 181-192.	3.0	24

Keiko Hattori

#	Article	IF	CITATIONS
55	Mantle wedge serpentinites: A transient reservoir of halogens, boron, and nitrogen for the deeper mantle. Geology, 2018, 46, 883-886.	4.4	24
56	Shoshonitic- and adakitic magmatism of the Early Paleozoic age in the Western Kunlun orogenic belt, NW China: Implications for the early evolution of the northwestern Tibetan plateau. Lithos, 2017, 286-287, 345-362.	1.4	23
57	Porphyry Copper Potential in Japan Based on Magmatic Oxidation State. Resource Geology, 2018, 68, 126-137.	0.8	23
58	Source and tectono-metamorphic evolution of mafic and pelitic metasedimentary rocks from the central Quetico metasedimentary belt, Archean Superior Province of Canada. Precambrian Research, 2004, 132, 155-177.	2.7	22
59	Eocene to Oligocene retrogression and recrystallization of the Stak eclogite in northwest Himalaya. Lithos, 2016, 240-243, 155-166.	1.4	21
60	Crustal-scale auriferous shear zones in the central Superior province, Canada. Geology, 1993, 21, 399.	4.4	20
61	Metasomatic origin of garnet orthopyroxenites in the subcontinental lithospheric mantle underlying Pali Aike volcanic field, southern South America. Mineralogy and Petrology, 2008, 94, 243-258.	1.1	20
62	Compositional variation and timing of aluminum phosphate-sulfate minerals in the basement rocks along the P2 fault and in association with the McArthur River uranium deposit, Athabasca Basin, Saskatchewan, Canada. American Mineralogist, 2015, 100, 1386-1399.	1.9	20
63	Tracing halogen and B cycling in subduction zones based on obducted, subducted and forearc serpentinites of the Dominican Republic. Scientific Reports, 2017, 7, 17776.	3.3	20
64	Mineralogy and origin of oxygen-bearing platinum-iron grains based on an X-ray absorption spectroscopy study. American Mineralogist, 2010, 95, 622-630.	1.9	18
65	The influence of metamorphic grade on arsenic in metasedimentary bedrock aquifers: A case study from Western New England, USA. Science of the Total Environment, 2015, 505, 1320-1330.	8.0	18
66	Characterizing fluids associated with the McArthur River U deposit, Canada, based on tourmaline trace element and stable (B, H) isotope compositions. Chemical Geology, 2017, 466, 417-435.	3.3	18
67	Longâ€lasting intracontinental strikeâ€slip faulting: new evidence from the Karakorum shear zone in the Himalayas. Terra Nova, 2011, 23, 92-99.	2.1	17
68	Geochemistry of ore deposition at the Yatani lead-zinc and gold-silver deposit, Japan. Economic Geology, 1975, 70, 677-693.	3.8	16
69	Origin of ultramafic xenoliths in high-Mg diorites from east-central China based on their oxidation state and abundance of platinum group elements. International Geology Review, 2012, 54, 1203-1218.	2.1	16
70	Identification of sandstones above blind uranium deposits using multivariate statistical assessment of compositional data, Athabasca Basin, Canada. Journal of Geochemical Exploration, 2018, 188, 229-239.	3.2	16
71	Protracted Magmatism and Mineralized Hydrothermal Activity at the Cibraltar Porphyry Copper-Molybdenum Deposit, British Columbia. Economic Geology, 2020, 115, 1119-1136.	3.8	16
72	Paragenesis and Composition of Tourmaline Types Along the P2 Fault and Mcarthur River Uranium Deposit, Athabasca Basin, Canada. Canadian Mineralogist, 2016, 54, 661-679.	1.0	15

Κεικό Ηάττορι

#	Article	IF	CITATIONS
73	Os-isotope study of platinum-group minerals in chromitites in Alpine-type ultramafic intrusions and the associated placers in Borneo. Mineralogical Magazine, 1992, 56, 157-164.	1.4	14
74	Oxidation state of lithospheric mantle along the northeastern margin of the North China Craton: implications for geodynamic processes. International Geology Review, 2013, 55, 1418-1444.	2.1	13
75	Metal binding to dissolved organic matter and adsorption to ferrihydrite in shallow peat groundwaters: Application to diamond exploration in the James Bay Lowlands, Canada. Applied Geochemistry, 2011, 26, 1649-1664.	3.0	12
76	Mineral Inclusions in Chromite from the Chromite Deposit in the Kudi Ophiolite, Tibet, Protoâ€Tethys. Acta Geologica Sinica, 2017, 91, 469-485.	1.4	12
77	Archean sulphur cycle: Evidence from sulphate minerals and isotopically fractionated sulphides in superior province, Canada. Chemical Geology: Isotope Geoscience Section, 1987, 65, 341-358.	0.6	11
78	Multivariate statistical analysis of the REE-mineralization of the Maw Zone, Athabasca Basin, Canada. Journal of Geochemical Exploration, 2016, 161, 98-111.	3.2	11
79	Geochemistry of peat over kimberlites in the Attawapiskat area, James Bay Lowlands, northern Canada. Applied Geochemistry, 2008, 23, 3767-3782.	3.0	10
80	Abyssal Serpentinites: Transporting Halogens from Earth's Surface to the Deep Mantle. Minerals (Basel, Switzerland), 2019, 9, 61.	2.0	9
81	Pyrite of distinctive isotopic composition from the Hemlo deposit: A potential tool to identify this type of gold mineralization in Archean terrain. Journal of Geochemical Exploration, 1987, 28, 85-102.	3.2	8
82	Diverse metal sources of Archaean gold deposits: evidence from in situ lead-isotope analysis of individual grains of galena and altaite in the Ross and Kirkland Lake deposits, Abitibi Greenstone belt, Canada. Contributions To Mineralogy and Petrology, 1993, 113, 185-195.	3.1	8
83	Late Archaean geological development recorded in the Timiskaming Group sedimentary rocks, Kirkland Lake area, Abitibi greenstone belt, Canada. Precambrian Research, 1994, 68, 23-42.	2.7	8
84	Provenance of igneous clasts in conglomerates of the Archaean Timiskaming Group, Kirkland Lake area, Abitibi greenstone belt, Canada. Canadian Journal of Earth Sciences, 1994, 31, 1749-1762.	1.3	8
85	Multielement statistical evidence for uraniferous hydrothermal activity in sandstones overlying the Phoenix uranium deposit, Athabasca Basin, Canada. Mineralium Deposita, 2018, 53, 493-508.	4.1	8
86	Protolith of the Stak eclogite in the northwestern Himalaya. Italian Journal of Geosciences, 2017, 136, 64-72.	0.8	8
87	In situ characterization of forearc serpentinized peridotite from the Sulu ultrahigh-pressure terrane: Behavior of fluid-mobile elements in continental subduction zone. Geoscience Frontiers, 2021, 12, 101139.	8.4	7
88	Meteoric hydrothermal origin of calcites in ?Green Tuff? formations, Miocene age, Japan. Contributions To Mineralogy and Petrology, 1980, 73, 145-150.	3.1	6
89	Negative ionization processes of osmium for isotopic measurements. International Journal of Mass Spectrometry, 1998, 176, 189-201.	1.5	6
90	The origin of Ti-oxide minerals below and within the eastern Athabasca Basin, Canada. American Mineralogist, 2020, 105, 1875-1888.	1.9	6

Keiko Hattori

#	Article	IF	CITATIONS
91	A multivariate statistical approach identifying the areas underlain by potential porphyry-style Cu mineralization, south-central British Columbia, Canada. Journal of Geochemical Exploration, 2019, 202, 13-26.	3.2	5
92	Thermotectonic events recorded by U-Pb geochronology and Zr-in-rutile thermometry of Ti oxides in basement rocks along the P2 fault, eastern Athabasca Basin, Saskatchewan, Canada. Bulletin of the Geological Society of America, 2022, 134, 567-576.	3.3	5
93	Geochemical processes in the formation of â€~forest rings': examples of reduced chimney formation in the absence of mineral deposits. Geochemistry: Exploration, Environment, Analysis, 2016, 16, 85-99.	0.9	4
94	Cumulates of arc magmas incorporated into the Sulu UHP metamorphic belt, eastern China. International Geology Review, 2016, 58, 703-718.	2.1	4
95	Metamorphosed Archean epithermal Au-As-Sb-Zn-(Hg) vein mineralization at the Campbell Mine, northwestern Ontario; discussion. Economic Geology, 1998, 93, 683-685.	3.8	4
96	Early Palaeozoic sub-arc chromitite-bearing peridotite in the Kudi ophiolite on the westernmost Tibetan Plateau. International Geology Review, 2019, 61, 1105-1123.	2.1	3
97	Zircon Chemistry and Oxidation State of Magmas for the Duobaoshan-Tongshan Ore-Bearing Intrusions in the Northeastern Central Asian Orogenic Belt, NE China. Minerals (Basel, Switzerland), 2021, 11, 503.	2.0	3
98	Spinel and Aspidolite from the Des Cèdres Dam Occurrence, Notre-Dame-du-Laus, Québec, Canada. Rocks and Minerals, 2016, 91, 448-452.	0.1	2
99	Evolution of lithospheric mantle beneath the Maguan region, southwestern margin of the South China block based on mantle xenoliths in Miocene alkaline volcanic rocks. Mineralogy and Petrology, 2021, 115, 173-192.	1.1	2
100	lgneous rocks related to porphyry <scp>Cuâ€Au</scp> mineralization at the Dizon mine, Philippines. Resource Geology, 2021, 71, 392-408.	0.8	2
101	Ultrahigh-Pressure Metamorphism and P-T Path of Xiaoxinzhuang Eclogites from the Southern Sulu Orogenic Belt, Eastern China, Based on Phase Equilibria Modelling. Minerals (Basel, Switzerland), 2022, 12, 216.	2.0	2
102	Petrogenesis of Garnet Clinopyroxenite and Associated Dunite in Hujialin, Sulu Orogenic Belt, Eastern China. Minerals (Basel, Switzerland), 2022, 12, 162.	2.0	1
103	Gold Mineralization in Izu Peninsula, Central Japan, during Crustal Extension in Response to Double Subduction. Resource Geology, 2019, 69, 167-175.	0.8	0
104	Ammonium abundance and short-wave infrared absorption spectra of altered rocks. Geochemistry: Exploration, Environment, Analysis, 2020, 20, 451-460.	0.9	0
105	Petrology of green polished stone axes of the Jomon period from the <scp>Sannaiâ€Maruyama</scp> site, Japan, investigating the origin of source rock. Island Arc, 2021, 30, e12384.	1.1	О